Molecular Science

AIMS Molecular Science, 10(3): 186–204.
DOI: 10.3934/molsci.2023013
Received: 22 May 2023
Revised: 08 August 2023
Accepted: 18 August 2023
Published: 28 August 2023

http://www.aimspress.com/journal/Molecular

Research article

Characterization of the human *IDH1* gene promoter

Yutaka Takihara[1], Ryuji Otani[1], Takuro Ishii[1], Shunsuke Takaoka[1], Yuki Nakano[1], Kaori Inoue[1], Steven Larsen[1], Yoko Ogino[1], Masashi Asai[1,2], Sei-ichi Tanuma[3] and Fumiaki Uchiumi[1,*]

[1] Department of Gene Regulation, Faculty of Pharmaceutical Sciences, Tokyo University of Science, Noda-shi, Chiba-ken 278-8510, Japan
[2] Department of Kampo Pharmacology, Faculty of Pharmaceutical Sciences, Yokohama University of Pharmacy, Yokohama-Shi, Kanagawa-ken 245-0066, Japan
[3] Genomic Medicinal Science, Research Institute for Science and Technology, Tokyo University of Science, Noda-shi, Chiba-ken 278-8510, Japan

* **Correspondence:** Email: f_uchiumi@rs.tus.ac.jp; Tel: +81471213616; Fax: +81471213608.

Abstract: In cancer, the production of ATP depends mainly on glycolysis, usually accompanied by the dysfunction of the tricarboxylic acid (TCA) cycle and oxidative phosphorylation (OXPHOS). Nicotinamide adenine dinucleotide (NAD^+) is a coenzyme for various biological enzymatic reactions such as those involved in the TCA cycle. To investigate the molecular mechanisms involved in carcinogenesis, the transcription system of genes associated with mitochondrial function should be elucidated. In this study, we isolated several mitochondrial function-associated bidirectional promoters and tested whether they responded to NAD^+-metabolism regulating compounds, namely, *trans*-resveratrol (Rsv), 2-deoxy-D-glucose (2DG), 3-amino benzamide (3AB), and olaparib (OLA), in HeLa S3 cells. Transient transfection and luciferase (Luc) reporter assay showed that the *IDH1* promoter was prominently activated by these compounds. The *IDH1* gene, which encodes a nicotinamide adenine dinucleotide phosphate ($NADP^+$) dependent isocitrate dehydrogenase, is frequently mutated in glioma and leukemia cells. In this study, RT-PCR showed that *IDH1* gene and protein expression was induced in response to the NAD^+-regulating drugs Rsv and 3AB. However, IDH1 protein amount was rather stable at control level. The result suggested that a post-transcriptional controlling system works to keep IDH1 at a stable level.

Keywords: bidirectional promoter; ETS; GGAA; IDH1; PARPi; resveratrol; transcription

1. Introduction

Generally, mitochondrial dysfunctions are observed in cancerous cells [1]. Furthermore, as we age, the risk of developing cancer increases. This is in contrast to decreasing levels of cellular NAD^+ [2]. Previously, it was shown that the cellular NAD^+/NADH ratio increases in response to *trans*-resveratrol (Rsv), 2-deoxy-D-glucose (2DG), 3-aminobenzamide (3AB) and olaparib (AZD2281) (OLA), in HeLa S3 cells [3]. A natural polyphenol, Rsv, which is contained in the skins of grapes, berries and peanuts, not only has an anticancer effect but also extends the life spans of various organisms [4]. Rsv is synthesized in plants in response to various environmental stresses such as fungal infection and UV irradiation [5,6]. Both *cis* and *trans* isomers are known, but biological activities are only reported for the *trans* isomer (3,5,4'-trihydroxy-*trans*-stilbene). Generally, Rsv is known to be beneficial for health, preventing obesity, diabetes and inflammatory and neurodegenerative diseases, affecting the cardiovascular system and a cancer-causing signaling pathway [7,8]. 2DG is a glucose derivative that limits glycolysis to induce autophagy [8]. The delay in cell proliferation without leading to severe cell death has been observed in clinical trials with 2DG [9]. Since 2DG inhibits glycolysis and nucleotide production, sensitivity to drugs and radiation could be induced [10]. 3AB resembles NAD^+ in structure and inhibits poly ADP-ribose (PAR) polymerase (PARP) [11,12], which localizes both in nuclei and mitochondria, playing essential roles in DNA repair, maintenance of the chromatin and cell survival. In the presence of DNA strand breaks, PARP binds to the breakage sites to synthesize PAR, consuming an NAD^+ as a substrate [13]. In normal cells, a homologous recombination system will help cells to survive. However, in cancerous cells that have *BRCA1* or *BRCA2* mutations, PARP inhibitors (PARPi) effectively induce cell death [14]. The first approved PARP inhibitor, OLA, induces autophagy and mitophagy in *BRCA* mutated ovarian and breast cancers to suppress proliferation [15]. PARPi are expected to reduce consumption of NAD^+ in PARP-activated cells.

In this study, the bidirectional promoters of the human mitochondrial function-associated genes were amplified by polymerase chain reaction (PCR). They were ligated into the multi-cloning site (MCS) of the Luc reporter plasmid pGL4.10[*luc*2]. Multiple transfection [16] and Luc assays in HeLa S3 cells showed that the *IDH1* promoter positively responded to all four NAD^+-affecting drugs. Quantitative RT-PCR and Western blotting showed that both gene and protein expressions of the *IDH1* were induced. Deletion and point mutation experiments narrowed the drug responsive region, containing duplicated GGAA and the GC-box. These findings suggested that up-regulation of NAD^+/NADH induces IDH1 to accelerate conversion of citrate to α-ketoglutarate, which could then be imported into mitochondria, assisting progression of the TCA cycle.

2. Materials and methods

2.1. Materials

Four compounds were tested if they could affect promoter activities. *trans*-Resveratrol (Rsv) (Cat. No. CAS501-36-0) [17] was purchased from Cayman Chemical (Ann Arbor, MI), and 2-deoxy-D-glucose (2DG) and 3-aminobenzamide (3AB) were purchased from WAKO Pure Chemical (Tokyo, Japan). Olaparib (OLA) was from ChemScene, LLC (Monmouth Junction, NJ). Rsv is known to upregulate mitochondrial complex I, which oxidizes NADH to produce NAD^+ [18]. 2DG has been also reported to increase cellular NAD^+/NADH level [19]. 3AB and OLA are well known as PARP

inhibitors [15,20]. It has been reported that NAD^+/NADH level in HeLa S3 cells could be upregulated by 8 h treatment of Rsv (20 μM), 2DG (8 mM), 3AB (5 mM), OLA (2.5 μM) [3].

2.2. Cells and cell culture

Human cervical carcinoma (HeLa S3) cells [16] were grown in Dulbecco's modified Eagle's medium (DMEM) (FUJIFILM Wako Pure Chemical, Osaka, Japan), supplemented with 10% fetal bovine serum (FBS) (Biosera, East Sussex, UK) and penicillin-streptomycin at 37 ℃ in a humidified atmosphere with 5% CO_2.

2.3. Construction of Luciferase (Luc) reporter plasmids

Various Luc reporter plasmids, carrying approximately 500 bp, which contain both transcription start sites (TSSs) of the human bidirectionally transcribed gene pairs (Figure 1), were constructed by a slight modification of the procedure that has previously been described [17,21].

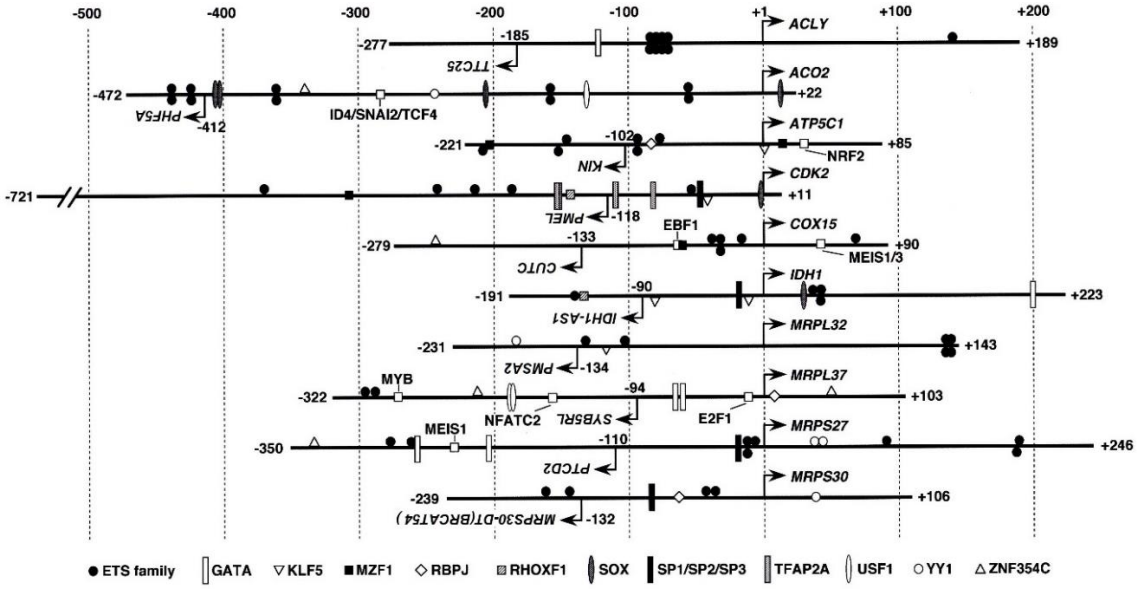

Figure 1. Mitochondrial function-associated gene promoters. The 5'-flanking regions of human mitochondrial function-associated genes, which were inserted into the MCS of the pGL4.10[*luc*2] vector, are shown. The TSSs or the 5'-ends of cDNAs are designated +1. These genes are head-head linked with bi-directional partner genes, which are transcribed from right to left. The JASPAR2018 program (threshold >98%) (http://jaspar.genereg.net/) was performed, and putative transcription factor binding elements are shown schematically.

Briefly, PCR was performed with sense/antisense primer-pair (Table 1) and genomic DNAs, which were extracted from HeLa S3 cells. The amplified DNA fragments, containing 466, 494, 306, 732, 369, 414 374, 425, 596 and 345 bp of the human *ACRY/TTC25*, *ACO2/PHF5A*, *ATP5C1/KIN*, *CDK2/PMEL*, *COX15/CUTC*, *IDH1/IDH-AS1*, *MRPL32/PMSA2*, *MRPL37/SYB5RL*, *MRPS327/PTCD2* and *MRPS30/MRPS30-DT* bidirectional promoter regions, were treated with

appropriate restriction enzyme(s). Then, they were ligated into the multi-cloning site (MCS) of pGL4.10[*luc*2] (Promega, Madison, WI). Resultant plasmids, containing the correct/(reverse) orientations, were named, as indicated in Table 1 and Figure 2.

Table 1. Primer pairs used for amplifying 5'-upstream regions of the human genes.

Luc plasmid	Primer	Sequence (5' to 3')
pGL4-IDH1	hIDH1-5914	TTCAAGCTTCGCTGTCGGGATTCGGGACTGAATCT
(pGL4-IDH1AS1)	AhIDH1-5502	TTTAAGCTTGGAGCCTGAGGTTACCTGCCGGGATG
pGL4-ACLY	hACLY-2813	TTCAAGCTTTAGAAAATTCCCCGCACAGGTAGAGC
(pGL4-TTC25)	AhACLY-2349	TTTAAGCTTACCACGTATGCCTCATCCCTATTCGG
pGL4-ACO2	hACO2-4533	TTCAAGCTTAGCCATAGCTCCTAACTAAGCCGGCC
(pGL4-PHF5A)	AhACO2-5033	GGGAAGCTTTGTGCACTGACAAAGATGAGGTCGCA
pGL4-ATP5C1	hATP5C1	ATCTCGAGTAAGAAAATCCGACTTCCCCAT
(pGL4-KIN)	AhATP5C1	ATCTCGAGAACATGGTAGCCACAGCCCTGC
pGL4-CDK2	hCDK2-5996	GGGAAGCTTAGCACCAGATCCATTGTGTTC
(pGL4-PMEL)	AhCDK2-6839	TTTAAGCTTGAAACAATGTTGCCGCCTCCC
pGL4-COX15	hCOX15-2379	TTCAAGCTTCGCTCAGAGGAGGCCCCCTGC
(pGL4-CUTC)	AhCOX15-2012	GGGAAGCTTCAAGGCCCTCAACGGCGGAAA
pGL4-CS	hCS-1991	ACAGGTACCTCCATGGCCGTGAAGCCATTAACC
	AhCS-1485	AAAAAGCTTGACAAGGTTGAAAGGAGGCGGCTG
pGL4-FH	hFH-6212	ACAGGTACCTATTTCATTATCTACACTTTGCTG
	AhFH-5730	AAAAAGCTTGGGTAGAATTTCTGGGCGGCTGTG
pGL4-MRPL32	hMRPL32-2004	CCCAAGCTTCCATACCTGAATGTAGTCAGC
(pGL4-PMSA2)	AhMRPL32-2482	CGGAAGCTTCCGTAGCAGTCGCTCCCAGTA
pGL4-MRPL37	hMRPL37-2096	TTTAAGCTTACAGCGAGGGACACTGGGCCT
(pGL4-CYB5RL)	AhMRPL37-2545	TTTAAGCTTGCGGGCCCGGACGCCAATGCC
pGL4-MRPS27	hMRPS27-0607	GGGAAGCTTAGGAGCTGTGGCTGCTCCACA
(pGL4-PTCD2)	AhMRPS27-0012	GGGAAGCTTGGGGTGTTTGGTAGTGCAGAA
pGL4-MRPS30	hMRPS30-8686	GGGAAGCTTGCCGTATAGGGTCCTACAAGT
(pGL4-BRCAT54)	AhMRPS30-9030	AAAAGCTTAGCCGCGGTGTGCAATGAAAG
pGL4-IDH3B	hIDH3B-5810	ACAGGTACCTGTCCTGGGGAGTTCAAGTCCGGG
	AhIDH3B-5192	AAAAAGCTTCTCCCGGGGCCTCACTCGGGTCAG
pGL4-IDH3G	hIDH3G-4814	TTTGGGTACCAACACCACCTGCCGTGGGTCAGAGG
	AhIDH3G-4327	CCCAAGCTTGACGGAAAGTGAGAGCCTCCGCACGT

Note: The names of Luc plasmids which PCR amplified DNA fragments were introduced in reverse orientations are indicated in the parentheses.

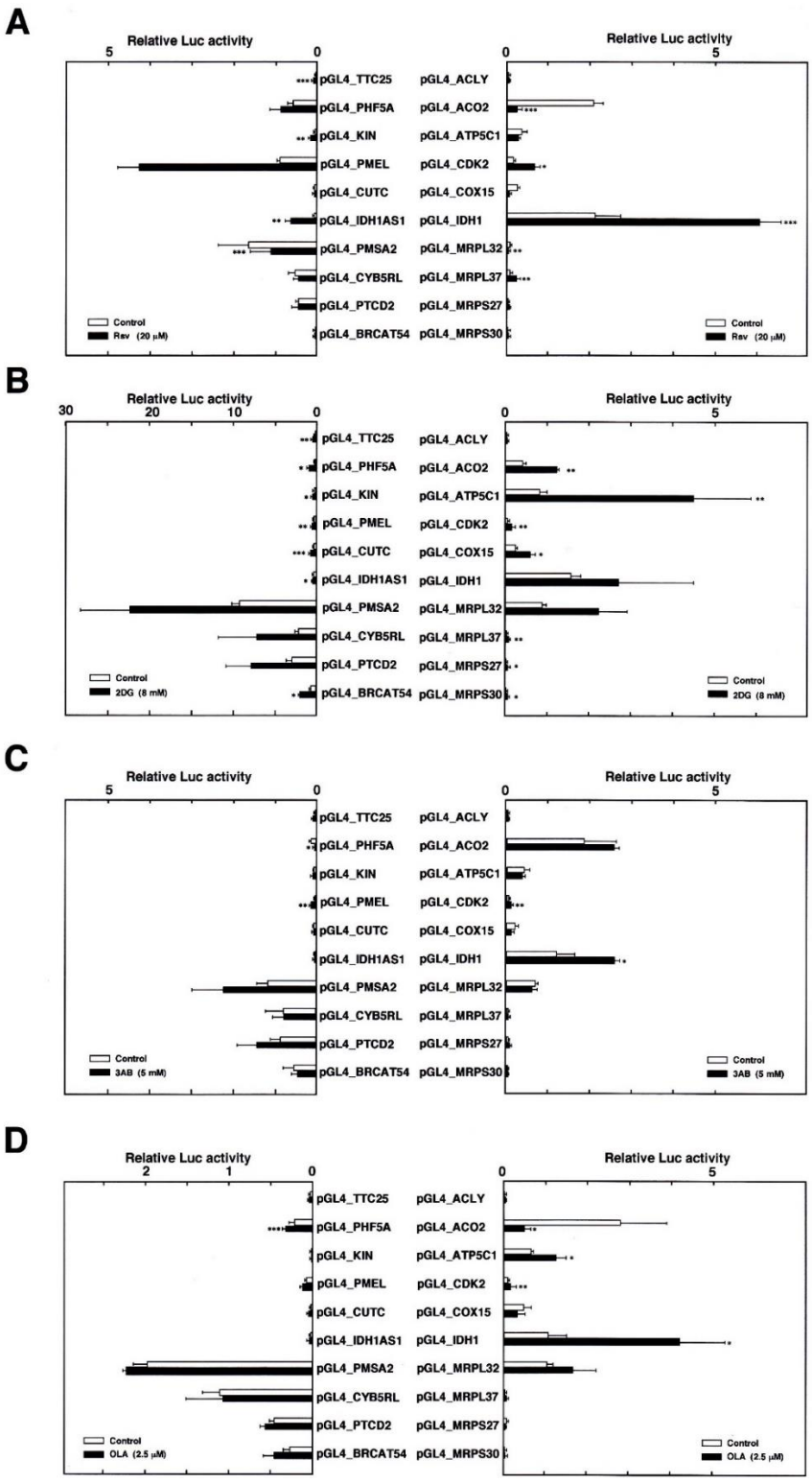

Figure 2. Effects of NAD^+ metabolism affecting drugs on mitochondrial function-associated genes in HeLa S3 cells. (A to D) The bidirectional promoter regions that contain putative TSSs of the human mitochondrial function-associated genes were inserted into the MCS of the pGL4.10[*luc*2] in both directions. The Luc reporter plasmids, containing 5'-upstream of mitochondrial function-associated genes (right panels) and oppositely transcribed genes (left panels), were transfected into HeLa S3 cells, which were treated

with Rsv (20 μM), 2DG (8 mM), 3AB (5 mM) or OLA (2.5 μM) for 24 h (A to D, respectively). Luc activities were normalized to that of the pGL4-PIF1 transfected and drug non-treated cells. Histograms show relative Luc activities compared with that of the control cells (treated with 0.05% DMSO). Results are shown as means ± S.D. from at least three independent experiments. Statistical analysis for the results between Rsv-treated and non-treated cells was performed with Student's *t*-test, and asterisks indicate values of *p<0.05, **p<0.01 and ***p<0.001.

Similarly, the *IDH1* promoter deletion-introduced plasmids were constructed by ligating a PCR-amplified DNA fragment into the MCS of pGL4.10[*luc*2]. pGL4-IDH1-414 has an identical region in the pGL4-IDH1, but the 5'-end of the inserted DNA has been designed to have a *Kpn*I site. The sense and anti-sense primers used for the amplification of the DNA fragments are shown in Table 2. The shaded nucleotides (Table 2) indicate the introduced mutations. PCR was performed with template pGL4-IDH1-WT and sense/antisense primer pairs, hIDH15180/AhIDH1-5084MM, hIDH15180M/AhIDH1-5084 and hIDH15180M/AhIDH1-5084MM (Table 2), to amplify mutation-introduced fragments, which were inserted into the MCS of pGL4.10[*luc*2] to make pGL4-IDH1-mut1, -mut2 and -mut3, respectively. The introduction of mutations in the pGL4-IDH1-mut4 and -mut5 was carried out according to a previously reported procedure [17] with slight modifications. Briefly, a PCR was carried out with sense hIDH1-mt/AhIDH1-mt primer pairs (Table 2) and pGL4-IDH1-mut1 as a template. The PCR products were denatured at 65 ℃ for 20 min, gradually cooled down to 25 ℃ for 20 min and further kept at 25 ℃ for 20 min. They were treated with T4 DNA polymerase (Toyobo, Osaka, Japan) and digested with *Kpn*I and *Xho*I, which were ligated into the MCS of the pGL4.10[*luc*2]. The pGL4-IDH1-mut5 was obtained by the same procedure using pGL4-IDH1-mut4 as a template for PCR. Nucleotide sequences were confirmed by a DNA sequencing service (FASMAC, Greiner Japan Inc., Atsugi, Japan) with primers Rv (TAGCAAAATAGGCTGTCCCC) and GL (CTTTATGTTTTTGGCGTCTTCC). The Luc reporter plasmids, pGL4-PIF1, were constructed as described [22].

2.4. Transient transfection and Luc assay

Luc reporter plasmids were transfected into HeLa S3 cells by DEAE-dextran method in 96-well plates [16], and after 24 h of transfection, the culture medium was changed to Rsv (20 μM), 2DG (8 mM), 3AB (5 mM) or OLA (2.5 μM) containing DMEM with 10% FBS. After a further 24 h of incubation, cells were collected and lysed with 100 μL of 1 × cell culture lysis reagent, containing 25 mM Tris-phosphate (pH 7.8), 2 mM DTT, 2 mM 1,2-diaminocyclohexane-N,N,N',N',-tetraacetic acid, 10% glycerol and 1% Triton X-100. They were mixed and centrifuged at 12,000 × g for 5 sec. The supernatant was stored at −80 ℃. The Luc assay was performed with a Luciferase assay system (Promega), and relative Luc activities were calculated as described previously [16,17,21,22]. Because the human *PIF* promoter (590 bp) [22], which is contained in the pGL4-PIF1, is not affected by all chemicals used, results were compared with the pGL4-PIF1-transfected cells after both control/chemicals addition.

Table 2. Primer pairs used for amplifying 5'-upstream regions of the human *IDH1* gene.

Luc plasmid	Primer	Sequence (5' to 3')
pGL4-IDH1-414	hIDH1-5334	TTCAAGCTTCGCTGTCGGGATTCGGGACTGAATCT
	AhIDH1-4921	TTTAAGCTTGGAGCCTGAGGTTACCTGCCGGGATG
pGL4-IDH1-D1	hIDH1-5215	TTTGGTACCTGACTCCGCCCATCCCACGGGAATTG
	AhIDH1-4921	GGGAAGCTTTGTGCACTGACAAAGATGAGGTCGCA
pGL4-IDH1-D2	hIDH1-5185	TTTGGTACCTGTGGCGATTGGAGGCGTGTCGGGGG
	AhIDH1-4921	AAAAAGCTTGACAAGGTTGAAAGGAGGCGGCTG
pGL4-IDH1-D3	hIDH1-5144	TTTGGTACCTGGGCTGAGGAGGCGGGGCCTGGGAG
	AhIDH1-4921	AAAAAGCTTGGGTAGAATTTCTGGGCGGCTGTG
pGL4-IDH1-D4	hIDH1-5109	TTTGGTACCCGGGAAGAGGAAAAGCTCGGACCTAC
	AhIDH1-4921	AAAAAGCTTCTCCCGGGGCCTCACTCGGGTCAG
pGL4-IDH1-D5	hIDH1-5083	TTTGGTACCCCTGTGGTCCCGGGTTTCTGCAGAGT
	AhIDH1-4921	GGGAAGCTTTGTGCACTGACAAAGATGAGGTCGCA
pGL4-IDH1-D6	hIDH1-5334	TTCAAGCTTCGCTGTCGGGATTCGGGACTGAATCT
	AhIDH1-4966	TTTAAGCTTGGGGCGCCACAGCCGCTCACAAGCTC
pGL4-IDH1-D7	hIDH1-5334	TTCAAGCTTCGCTGTCGGGATTCGGGACTGAATCT
	AhIDH1-5031	TTGAAGCTTCCCAGTGCCTCCGCTTCTGAAGTAGA
pGL4-IDH1-D8	hIDH1-5334	TTCAAGCTTCGCTGTCGGGATTCGGGACTGAATCT
	AhIDH1-5110	TTTAAGCTTTGTCCCCTCCCAGGCCCCGCCTCCTC
pGL4-IDH1-D9	hIDH1-5334	TTCAAGCTTCGCTGTCGGGATTCGGGACTGAATCT
	AhIDH1-5145	TTTAAGCTTCCTCCCCCAGCCCCGCCCCCGACACG
pGL4-IDH1-D10	hIDH1-5334	TTCAAGCTTCGCTGTCGGGATTCGGGACTGAATCT
	AhIDH1-5185	TTTAAGCTTACGCCAATTCCCGTGGGATGGGCGGA
pGL4-IDH1-D11	hIDH1-5185	TTTGGTACCTGTGGCGATTGGAGGCGTGTCGGGGG
	AhIDH1-5031	TTGAAGCTTCCCAGTGCCTCCGCTTCTGAAGTAGA
pGL4-IDH1-D12	hIDH1-5185	TTTGGTACCTGTGGCGATTGGAGGCGTGTCGGGGG
	AhIDH1-5110	TTTAAGCTTTGTCCCCTCCCAGGCCCCGCCTCCTC
pGL4-IDH1-D13	hIDH1-5144	TTTGGTACCTGGGCTGAGGAGGCGGGGCCTGGGAG
	AhIDH1-5031	TTGAAGCTTCCCAGTGCCTCCGCTTCTGAAGTAGA
pGL4-IDH1-D14	hIDH1-5144	TTTGGTACCTGGGCTGAGGAGGCGGGGCCTGGGAG
	AhIDH1-5110	TTTAAGCTTTGTCCCCTCCCAGGCCCCGCCTCCTC
pGL4-IDH1-WT	hIDH1-5180	TAAGGTACCGATTGGAGGCGTGTCGGGGGCGGGGC
	AhIDH1-5084	CCCAAGCTTAGGTCCGAGCTTTTCCTCTTCCCGGC
pGL4-IDH1-mut1	hIDH1-5180	TAAGGTACCGATTGGAGGCGTGTCGGGGGCGGGGC
	AhIDH1-5084MM	CCCAAGCTTAGGTCCGAGCTTTTGGTCTTGGCGGC
pGL4-IDH1-mut2	hIDH1-5180M	TAAGGTACCGATTGGAGGCGTGTCGGTGTCGTGGC
	AhIDH1-5084	CCCAAGCTTAGGTCCGAGCTTTTCCTCTTCCCGGC
pGL4-IDH1-mut3	hIDH1-5180M	TAAGGTACCGATTGGAGGCGTGTCGGTGTCGTGGC
	AhIDH1-5084MM	CCCAAGCTTAGGTCCGAGCTTTTGGTCTTGGCGGC
pGL4-IDH1-mut4	hIDH1-mt	GGAGGTGGGCTGAGGATGCTGTGCCTGGGAGGGGA
pGL4-IDH1-mut5	AhIDH1-mt	GCTTTGTCCCCTCCCAGGCACAGCATCCTCAGCCC

Note: Shaded characters indicate mutations that were introduced into Luc reporter plasmids.

2.5. Western blot analysis

Western blot analysis was carried out after SDS-PAGE (15% acrylamide) as previously described [17,21], with antibodies against IDH1 (Cat. No. sc-49996, Santa Cruz Biotechnology, Santa Cruz, CA) and β-actin (Cat. No. A5441, Sigma-Aldrich, St Louis, MO) followed by the addition of horseradish peroxidase (HRP)-conjugated anti goat (Cat. No. HAF109, Bio-techne, Minneapolis, MN) or anti-mouse IgG (Cat. No. A9917, Sigma-Aldrich, St Louis, MO) secondary antibodies. Signal intensities were quantified with a ChemiDoc and Image Lab system (Bio-Rad, Berkeley, CA).

2.6. Quantitative real-time reverse transcriptase polymerase chain reaction (RT-qPCR)

First-strand cDNAs were synthesized with ReverTra Ace (Toyobo, Tokyo, Japan), random primers (Takara) and total RNAs extracted from HeLa S3 cells. Real time PCR analysis was carried out using the Mx3000P Real-Time qPCR System (Stratagene, La Jolla, CA) [17,21]. For PCR amplification, cDNAs were amplified by Thunderbird Realtime PCR Master Mix (Toyobo) and 0.3 μM of each primer pair. The primer pairs for amplifying human *IDH1* and *GAPDH* transcripts were IDH1_h1104 GCATAGGCTCATCGACGACA/IDH1_Ah1236 CATCATGCCGAGAGAGCCAT and hGAPDH556/hGAPDH642 [17,21,22], respectively. Amplification was carried out initially for 1 min at 95 ℃, followed by 40 cycles (95 ℃ 15 sec and 58 ℃ 30 sec). Quantitative PCR analysis for each sample was carried out in triplicates. Relative gene expression values were obtained by normalizing C_T (threshold cycle) values of target genes in comparison with C_T values of the *GAPDH* gene using the $\Delta\Delta C_q$ method [23].

2.7. Statistical analysis

Standard deviations (S.D.) for each data were calculated and results are shown as means ± S.D. from three independent experiments. Statistical analysis for data in Figures 2, 3, and 7 was performed with the Student *t*-test, and asterisks indicate values of $*p < 0.05$, $**p < 0.01$ and $***p < 0.001$.

3. Results

3.1. Confirmation of bidirectional promoters that contain mitochondrial function associated gene transcription start sites by comparison of NCBI database

Duplicated GGAA motifs are frequently found within 500 bp from the putative TSSs of mitochondrial function associating protein-encoding genes [24]. To examine whether they respond to NAD^+/NADH ratio-upregulating drugs [3], we cloned 306 to 732 bp of the 5′ upstream regions of the *ACO2, ACLY, IDH1, ATP5C1, COX15, CDK2, MRPL32, MRPL37, MRPS27* and *MRPS30* genes (Figure 1). As indicated, these genes are head-head linked with other genes or TSSs of non-coding RNAs. The JASPAR database indicated that most of them contained duplicated GGAA (TTCC) motifs.

The *IDH1* promoter responded to Rsv, 2DG, 3AB and OLA (Figure 2A–D, respectively), which are known to induce cellular NAD^+/NADH level after 8 h treatment of HeLa S3 cells [3]. The enzymes IDH3B, IDH3G, ACO2, CS and FH catalyzed reactions of the TCA cycle [25–27]. The duplicated GGAA (TTCC) motifs are contained in the cloned 5'-upstream regions of the *IDH3B*, *ACO2*, *CS* and

FH genes (Figure 3). Similar experiments showed that *IDH3B*, *IDH3G*, *ACO2*, *CS* and *FH* promoters respond to 2DG and other drugs (Figures 2 and 3). Among them, only the *IDH1* promoter showed positive responses to all drugs tested. Therefore, we focused on the regulation system of the *IDH1* gene expression in HeLa S3 cells. Sequence analysis revealed that the PCR-amplified 414 bp of the pGL4-IDH1-414 contains a nucleotide identical to NCBI Sequence ID NC_000002.12 (nucleotide from 208255334 to 208254921) and that it covers the sequence of the most-upstream 5'- end of the *IDH1* cDNA (Sequence ID NM_005896.3 and GENE ID 3417) having no mutations. This 414 bp contains a 5'-upstream end of a non-coding RNA (ncRNA) *IDH1-AS1* (Sequence ID NR_046452.1 and GENE ID 100507475) in a reverse orientation to that of the *IDH1* gene. The TSS was tentatively set as +1 at the most upstream 5' of the *IDH1* transcripts shown in the database. The JASPAR database (http://jaspar.genereg.net/) suggested several known transcription factor recognition sequences (Figure 4). Although no obvious TATA or CCAAT boxes were found, putative binding sites for E2F1 (-158 to -148), ETS1 (+43 to +48), GATA2 (-61 to -57, +195 to +199), KLF5 (-20 to -11, -87 to -78, +20 to +29), KLF14 (-88 to -75), KLF16 (-21 to -11, -87 to -77), MZF1 (-153 to -138, -9 to -4), NFIC (-48 to -43, +128 to +133), NFIX (+126 to +134), RHOXF1 (-134 to -127), SOX10 (+29 to +34), SP1 (-21 to -11, +8 to +18), SP2 (+4 to +18), SP3 (-87 to -77, -21 to -11), SPI1 (-145 to -140, +37 to +42) and SPIB (+41 to +47) are contained.

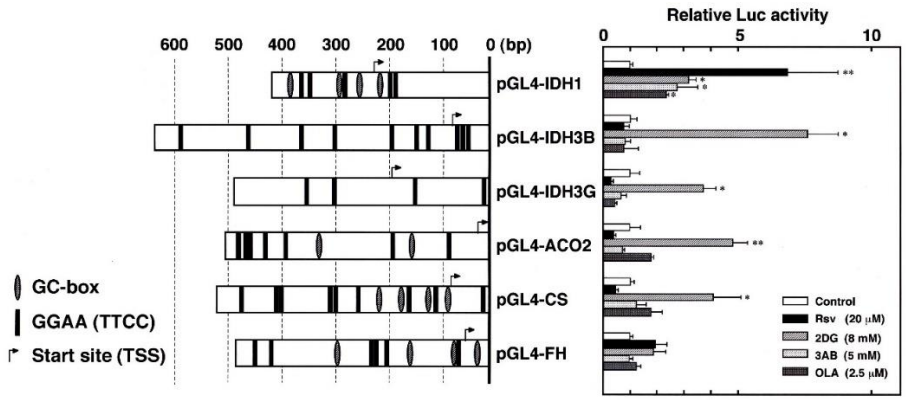

Figure 3. Effects of Rsv, 2DG, 3AB and OLA on promoter activities of the genes that encode human TCA cycle enzymes. (Left panel) The 5'-upstreams of the human TCA cycle enzyme encoding genes, which have been ligated into the MCS of the pGL4.10[*luc*2], are shown. The putative TSSs are indicated by arrows. GC-boxes and GGAA (TTCC) motifs are schematically shown. Luc reporter plasmids were transiently transfected into HeLa S3cells and treated with Rsv (20 μM), 2DG (8 mM), 3AB (5 mM) or OLA (2.5 μM) for 24 h. Luc activities were normalized to that of the pGL4-PIF1 transfected cells. Histograms show relative Luc activities compared with that of the same plasmid transfected cells without drug treatment. Statistical analysis for the results between Rsv-treated and non-treated cells was performed with Student's *t*-test, and asterisks indicate values of *$p < 0.05$ and **$p < 0.01$.

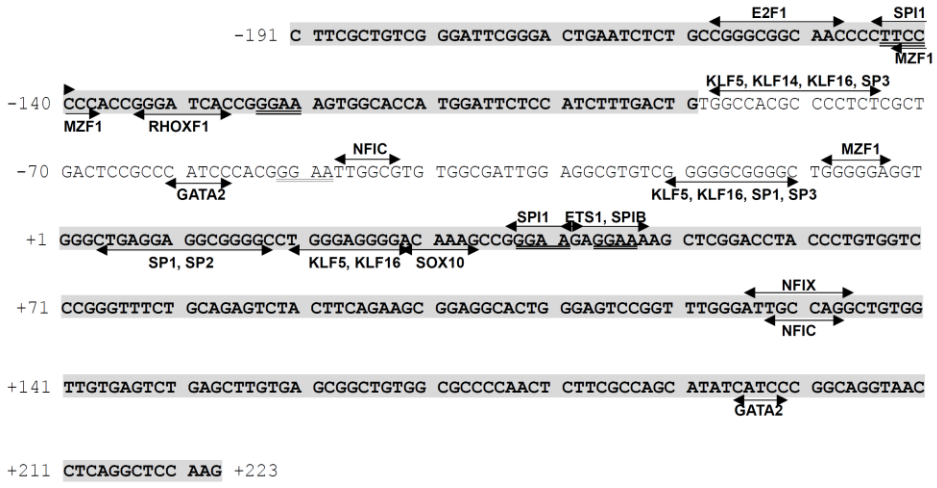

Figure 4. The 5'-upstream sequence of the human *IDH1* gene. The nucleotide sequence of the PCR-amplified 414 bp is shown. The human *IDH1* cDNA (NM_005896.3) and *IDH1-AS1* (NR_046452.1) are indicated by bold and shaded characters, respectively. The most upstream of the *IDH1* cDNA is numbered as nucleotide +1. Putative transcription factor-binding sites (JASPAR2018 program, threshold > 95%) are indicated by arrows.

3.2. Effects of Rsv on IDH1 gene expression and its protein amount in HeLa S3 cells

First, total RNAs were extracted from cells after adding Rsv (20 μM) to the culture medium. The relative gene expression *IDH1*/*GAPDH* began to increase from 1 h after Rsv addition and reached a transient peak at 2 h, and then it declined and gradually increased to 2-fold at 24 h (Figure 5).

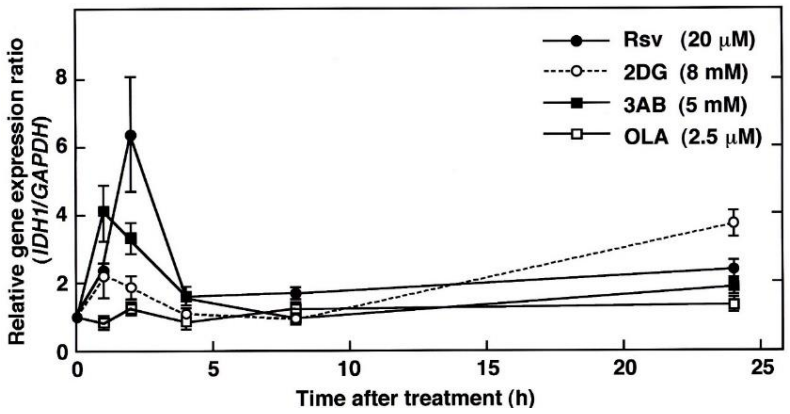

Figure 5. RT-qPCR analysis of the *IDH1* transcripts in HeLa S3 cells. The culture medium of HeLa S3 cells was changed to DMEM containing 10% FBS and indicated drugs. Cells were harvested after 0, 2, 4, 8 and 24 h of the treatment. Total RNAs were extracted from cells, and synthesized cDNAs were subjected to real time quantitative PCR with primer pairs to amplify *IDH1* and *GAPDH* cDNA. The results show the relative *IDH1/GAPDH* gene expression ratio compared with that of the non-drug-treated cells. Results are shown as means ± S.D. from at least three independent experiments.

3AB (5 mM) treatment also induced relative *IDH1* gene expression after 1 to 2 h addition to the culture medium (Figure 5). Similar early response was observed by 2DG (8 mM) treatment. However, the effect was most eminent at 24 h after the treatment. Surprisingly, OLA (2.5 μM) did not affect the *IDH1* gene expression during 24 h treatment. The results suggested that 2DG and OLA evoked some signals that regulate *IDH1* transcripts degradation or splicing. The observations, indicating that Rsv and 3AB increased *IDH1* transcripts effectively early after the treatment, lead us to further analyze IDH1 protein amount. However, Western blot analysis revealed that the amount of IDH1 protein did not change significantly during treatment with Rsv and 3AB. The IDH1/β-actin ratio was reduced to 85% of the control after 2 h, but it increased to the control level at 4 h after Rsv treatment, and then it declined and increased again to the control level (Figure 6). The IDH1/β-actin ratio did not change during 3AB treatment (Figure 6). The results suggest that the amount of IDH1 protein is restricted or post-transcriptionally maintained at a stable level through two mechanisms: degradation of IDH1 protein and regulation by non-coding or micro RNAs with regulatory functions.

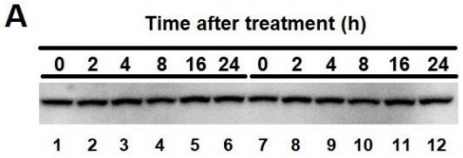

C

Time after treatment (h)	0	2	4	8	16	24
RSV (20 μM)	1.000	0.852	1.010	0.857	0.920	1.000
3-AB (5 mM)	1.000	0.990	0.917	0.939	0.806	0.993

Figure 6. Western blot analysis of the IDH1 protein in HeLa S3 cells. HeLa S3 cells that were treated with (A and B) Rsv (20 μM) (lanes 1-6) or 3AB (5 mM) (lanes 7-12) were collected after 0, 2, 4, 8, 16 and 24 h. Then extracted proteins were separated by a 15% SDS-PAGE, and Western blotting was performed with primary antibodies against IDH1 and β-actin (A and B, respectively). (C) Each band was quantified, and the results show the relative IDH1/β-actin protein expression ratio.

3.3. Identification of a drug responsive element in the IDH1 promoter

To narrow the drug responsive sequence(s), deletion was introduced in the pGL4-IDH1-414 plasmid vector (Figure 7A). Positive responses to 2DG, 3AB and OLA were observed in pGL4-IDH1-Δ1 and -Δ2-transfected cells. However, pGL4-IDH1-Δ3-transfected cells showed a much-lowered response to Rsv compared to the pGL4-IDH1-Δ2-transfected cells (Figure 7A).

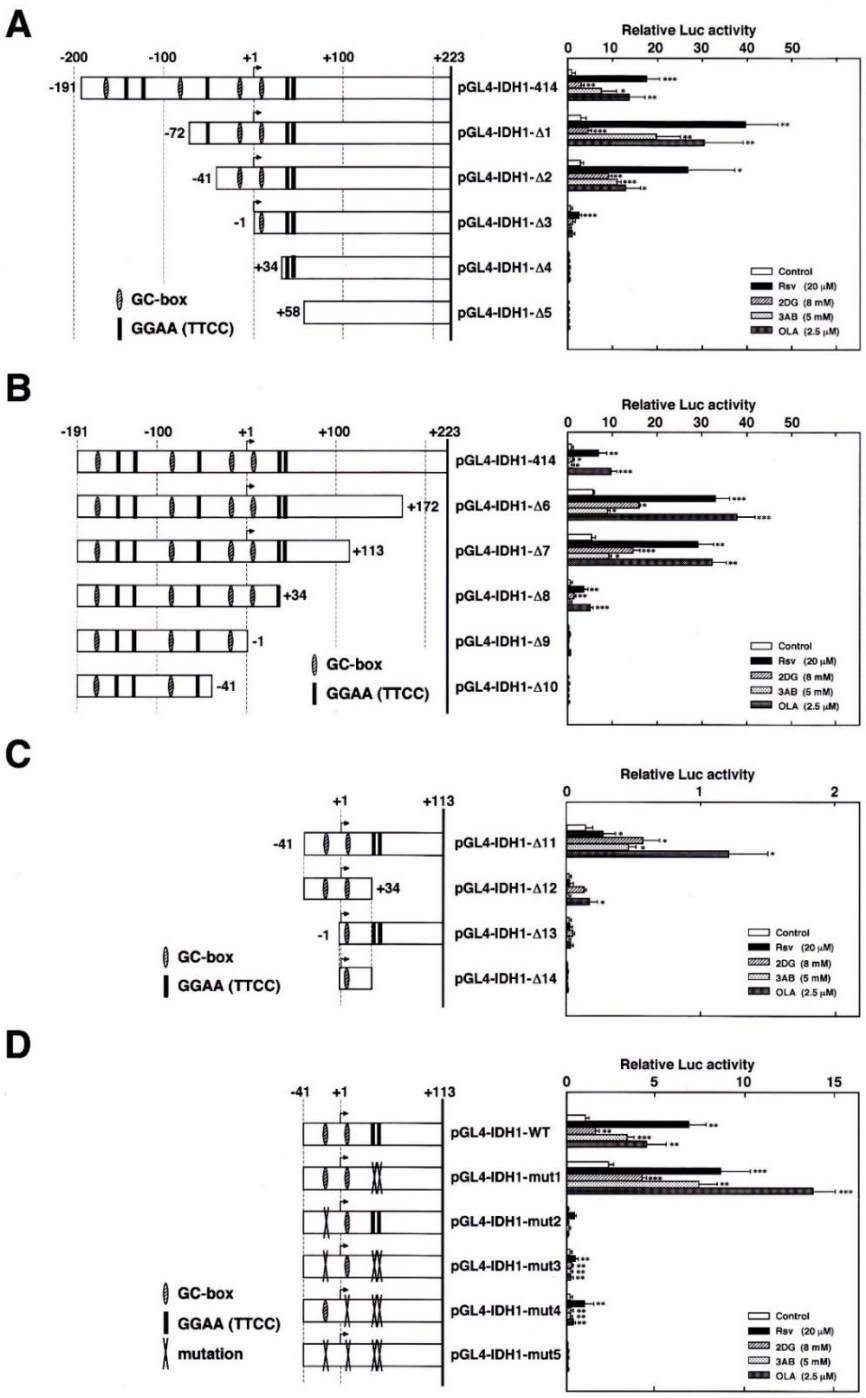

Figure 7. Drug response element in the human *IDH1* promoter. (Left panels) The *IDH1* promoter regions in the Luc expression construct are schematically indicated. Deletions from (A) 5'-end and (B) 3'-end of the 414 bp *IDH1* promoter region were introduced. (D) Mutations were introduced in the 154 bp human *IDH1* minimum promoter region. (A to D) Luc reporter plasmids were transiently transfected into HeLa S3 cells and treated with drugs for 24 h. Luc activities were normalized to that of the pGL4-PIF1 transfected cells. Results are shown as means ± S.D. from three independent experiments. Statistical analysis of the results between Rsv-treated and non-treated cells was performed with Student's *t*-test, and asterisks indicate values of *$p < 0.05$, **$p < 0.01$ and ***$p < 0.001$.

The pGL4-IDH1-Δ8-transfected cells showed apparent responses to all drugs (Figure 7B), but this was not observed in pGL4-IDH1-Δ9 transfected cells, suggesting the 35 bp containing the putative c-ETS binding sequence and a GC-box are of primary importance for *IDH1* promoter activity. This was confirmed by further deletion experiments, showing that a 154 bp sequence from -41 to +113 is a core promoter region with drug responsiveness (Figure 7C). This core promoter sequence is thought to be conserved within mammals, because the BLAST search program indicated that upstream sequence 153 bp region of the mouse *Idh1* gene transcript variant 2 (in NC_000067.7) has 71% homology with the 154 bp (in NC_000002.12) (supplementary Figure 1). To precisely indicate the drug responsive element(s), point mutations were introduced to the pGL4-IDH1-WT that carries the 154 bp (Figure 7D). Mutations on a GC-box (in pGL4-IDH1-mut2) greatly reduced basal promoter activity and the response to the drugs. The pGL4-IDH1-mut1-transfected cells showed higher promoter activity than pGL4-IDH1-WT transfected cells, suggesting that the duplicated GGAA functions as a suppressor or a modulator. The positive responses to drugs were completely lost by a mutation on the GC-box in the pGL4-IDH1-mut4 and -mut5 (Figure 7D). These results suggested that the *IDH1* promoter is co-operatively regulated by the c-ETS element and a GC-box to respond to NAD^+ up-regulating drugs in HeLa S3 cells.

4. Discussion

Many interferon-stimulated genes (ISGs) [28] and DNA repair-factor encoding genes [29] are TATA-less [30]. The human *E2F4* [21] and *ZNFX1* [31] promoters are also TATA-less, containing duplicated GGAA-motifs to respond to TPA, which induces macrophage-like differentiation of HL-60 cells. Moreover, duplicated GGAAs are contained in the human *TP53* [17], *HELB* [32] and *MCM4* [33] and a variety of mitochondrial function-associated gene promoters [29]. The *ACLY*, *ACO2*, *IDH1* and *ATP5C1* encode enzymes that regulate or affect the TCA cycle [34] or OXPHOS [35]. The *MRPL32*/*37*, *MRPS27*/*30* and *PTCD2* genes encode mitochondrial ribosomal protein subunits [36] and a regulator that processes the RNA of cytochrome b [37]. All tested promoters containing duplicated GGAAs responded to 8 mM of 2DG (Figure 2), which limits glucose uptake and hexokinase activity [38] and up-regulates NAD^+/NADH ratio in HeLa S3 cells [19]. Rsv activates mitochondrial complex I in the respiratory system [18]. 3AB and OLA will increase NAD^+ by inhibiting PARP that consumes NAD^+ for PAR synthesis [12]. Generally, in cancerous cells, energy production primarily depends on glycolysis [39]. Lowered NAD^+/NADH ratio, during aging and cancer development [40], may cause both the Warburg effect and mitochondrial dysfunction. In this study, it was strongly suggested that the *IDH1* promoter contains NAD^+/NADH sensitive element(s). However, the protein amount of IDH1 should be tightly regulated (Figure 6) by post-transcriptional mechanisms, which should be elucidated. It has been reported that miR-181a in mouse [41] and miR-32/-92b in human breast cancer [42] reduce IDH1. In addition, miR-101 and miR-183 could suppress IDH2 in human cancer [43,44]. Although expression of micro RNAs in HeLa S3 cells has not been examined, they could target IDH1 and IDH2. Generally, the upregulation of the NAD^+/NADH ratio is thought to be beneficial for cancer prevention and anti-aging. Anyhow, the results all suggest that if an NAD^+/NADH increasing event happens, post-transcriptional regulation will prevent aberrant increase of IDH1, which could be involved in fatty acid metabolism [45].

SP1, SP3, KLF5 and KLF16 bind to GC-box [46], which is present adjacent to the putative TSS of the *IDH1* gene (Figure 4). The Sp1 and KLF5 induce *HIF-1* gene expression [47-49]. In this study,

it was shown that the GC-box is essential for the drug response, and a duplicated GGAA motif acts as a suppressor (Figure 7D). ETS family proteins and NF-κB, which bind to duplicated GGAA containing sequences [50], might hinder other TFs' action. Given that CtBP regulates mitochondrial function [51,52] by binding to SPI1 and NF-κB [53,54], it can regulate NAD^+-dependent transcription.

In cancer, NAD^+ would be consumed by PARP when DNA damage occurs. In gliomas and glioblastomas, increased cellular NAD^+, which causes high *IDH1* expression [55], may increase NADPH that activates hypoxia-inducible factor-1 (HIF-1) to promote hypoxia [48,56]. Under such circumstances, both lipid biosynthesis and hypoxia will be overpromoted to disturb the oxidation/reduction balance, forcing cells into a malignant state [57]. NAD^+, which is reduced in accordance with aging [40], is an essential co-enzyme for the TCA cycle and OXPHOS and suppresses carcinogenesis [57,58]. It should be noted that IDH1 plays a role in epigenetic regulation [59] and that its gene promoter is bidirectional, linked with *IDH1-AS1* in a head-head manner. In contrast, promoters of the *DNMT1*, *DNMT3A*, *DNMT3B* and *DNMT3L* genes, which encode DNA methyl transferases, are unidirectional to be isolated from other gene TSSs. NAD^+ dependent deacetylase SIRT1 prevents DNA methylation in murine embryonic stem cells [60]. To establish a novel mitochondrial metabolism targeting [61,62] anti-cancer gene therapy [63], the NAD^+ dependent transcriptional and post-transcriptional systems should be elucidated.

Use of AI tools declaration

The authors declare they have not used Artificial Intelligence (AI) tools in the creation of this article.

Acknowledgments

The authors are grateful to Kohei Hoshino, Yuka Iinuma and Yutaka Yamamoto for excellent technical assistance. This study was performed under the permission of the recombinant DNA experimental committee admission No 1754 of the Tokyo University of Science. The present study was supported in part by JSPS KAKENHI grant no. 24510270 and a Research Fellowship from the Research Center for RNA Science, RIST, Tokyo University of Science.

Conflict of interest

Fumiaki Uchiumi is an editorial board member for AIMS Molecular Science and was not involved in the editorial review or the decision to publish this article.

The authors declare that they have no competing interests.

References

1. Seyfried TN Cancer as a mitochondrial metabolic disease*Front Cell Dev Biol* 3: 43. https://doi.org/10.3389/fcell.2015.00043
2. Yaku K, Okabe K, Nakagawa T (2018) NAD metabolism: Implications in aging and longevity. *Ageing Res Rev* 47: 1–17. https://doi.org/10.1016/j.arr.2018.05.006

3. Takihara Y, Sudo D, Arakawa J, et al. (2018) Nicotinamide adenine dinucleotide (NAD^+) and cell aging. In: *New research on cell aging and death*, 131–158. Available from: https://novapublishers.com/wp-content/uploads/2018/11/978-1-53613-626-5_short_commentary.pdf
4. Stefani M, Markus MA, Lin RCY, et al. (2007) The effect of resveratrol on a cell model of human aging. *Ann NY Acad Sci* 1114: 407–418. https://doi.org/10.1196/annals.1396.001
5. Saiko P, Szakmary A, Jaeger W, et al. (2008) Resveratrol and its analogs: defense against cancer, coronary disease and neurodegenerative maladies or just a fad? *Mutat Res/Rev Mutat Res* 658: 68–94. https://doi.org/10.1016/j.mrrev.2007.08.004
6. Kundu JK, Surh YJ (2008) Cancer chemopreventive and therapeutic potential of resveratrol: Mechanistic perspectives. *Cancer Lett* 269: 243–261. https://doi.org/10.1016/j.canlet.2008.03.057
7. Pezzuto JM (2008) Resveratrol as an inhibitor of carcinogenesis. *Pharm Biol* 46: 443–573. https://doi.org/10.1080/13880200802116610
8. Jang M, Cai L, Udeani GO, et al. (1997) Cancer chemopreventive activity of resveratrol, a natural product derived from grapes. *Science* 275: 218–220. https://doi.org/10.1126/science.275.5297.218
9. Ben Sahra I, Laurent K, Giuliano S, et al. (2010) Targeting cancer cell metabolism: The combination of metformin and 2-deoxyglucose induces p53-dependent apoptosis in prostate cancer cells. *Cancer Res* 70: 2465–2475. https://doi.org/10.1158/0008-5472.CAN-09-2782
10. Raez LE, Papadopoulos K, Ricart AD, et al. (2013) A phase I dose-escalation trial of 2-deoxy-D-glucose alone or combined with docetaxel in patients with advanced solid tumors. *Cancer Chemother Pharmacol* 71: 523–530. https://doi.org/10.1007/s00280-012-2045-1
11. Inal V, Mas MR, Isik AT, et al. (2015) A new combination therapy in severe acute pancreatitis—hyperbaric oxygen plus 3-Aminobenzamide. *Pancreas* 44: 326–330. http://doi.org/10.1097/MPA.0000000000000240
12. Meng X, Song W, Deng B, et al. (2015) 3-aminobenzamide, one of poly (ADP-ribose) polymerase-1 inhibitors, rescues apoptosis in rat models of spinal cord injury. *Int J Clin Exp Pathol* 8: 12207–12215.
13. Tanuma S, Sato A, Oyama T, et al. (2016) New insights into the roles of NAD^+-poly(ADP-ribose) metabolism and poly(ADP-ribose) glycohydrolase. *Curr Protein Pep Sci* 17: 668–682. https://doi.org/10.2174/1389203717666160419150014
14. Jiang X, Li X, Li W, et al. (2019) PARP inhibitors in ovarian cancer: Sensitivity prediction and resistance mechanisms. *J Cell Mol Med* 23: 2303–2313. https://doi.org/10.1111/jcmm.14133
15. Arun B, Akar U, Gutierrez-Barrera AM, et al. (2015) The PARP inhibitor AZD2281 (Olaparib) induces autophagy/mitophagy in BRCA1 and BRCA2 mutant breast cancer cells. *Int J Oncol* 47: 262–268. https://doi.org/10.3892/ijo.2015.3003
16. Uchiumi F, Larsen S, Tanuma S (2014) Application of DEAE-dextran to an efficient gene transfer system. In: *Dextran: Chemical structure, application and potential side effects*, 143–156. Available from: http://novapublishers.com/wp-content/uploads/2019/05/978-1-62948-960-5_ch5.pdf
17. Uchiumi F, Shoji K, Sasaki Y, et al. (2016) Characterization of the 5'-flanking region of the human *TP53* gene and its response to the natural compound, Resveratrol. *J Biochem* 159: 437–447. https://doi.org/10.1093/jb/mvv126

18. Desquiret-Dumas V, Gueguen N, Leman G, et al. (2013) Resveratrol induces a mitochondrial complex I-dependent increase in NADH oxidation responsible for sirtuin activation in liver cells. *J Biol Chem* 288: 36662–36675. https://doi.org/10.1074/jbc.M113.466490
19. Di LJ, Fernandez AG, de Siervi A, et al. (2010) Transcriptional regulation of BRCA1 expression by a metabolic switch. *Nat Struct Mol Biol* 17: 1406–1413. https://doi.org/10.1038/nsmb.1941
20. Herceg Z, Wang ZQ (1999) Failure of poly(ADP-ribose) polymerase cleavage by caspases leads to induction of necrosis and enhanced apoptosis. *Mol Cell Biol* 19: 5124–5133. https://doi.org/10.1128/MCB.19.7.5.5124
21. Hamada H, Goto Y, Arakawa J, et al. (2019) Characterization of the human *E2F4* promoter region and its response to 12-*O*-tetradecanoylphorbol-13-acetate. *J Biochem* 166: 363–373. https://doi.org/10.1093/jb/mvz047
22. Uchiumi F, Watanabe T, Tanuma S (2010) Characterization of various promoter regions of the human DNA helicase-encoding genes and identification of duplicated *ets* (GGAA) motifs as an essential transcription regulatory element. *Exp Cell Res* 316: 1523–1534. https://doi.org/10.1016/j.yexcr.2010.03.009
23. Livak KJ, Schmittgen TD (2001) Analysis of relative gene expression data using real-time quantitative PCR and the $2^{-\Delta\Delta CT}$ method. *Methods* 25: 402–408. https://doi.org/10.1006/meth.2001.1262
24. Uchiumi F, Fujikawa M, Miyazaki S, et al. (2014) Implication of bidirectional promoters containing duplicated GGAA motifs of mitochondrial function-associated genes. *AIMS Mol Sci* 1: 1–26. https://doi.org/10.3934/molsci.2013.1.1
25. Krell D, Assoku M, Galloway M, et al. (2011) Screen for *IDH1, IDH2, IDH3, D2HGDH* and *L2HGDH* mutations in glioblastoma. *PLoS One* 6: e19868. https://doi.org/10.1371/journal.pone.0019868
26. Cai Q, Zhao M, Liu X, et al. (2017) Reduced expression of citrate synthase leads to excessive superoxide formation and cell apoptosis. *Biochem Biophys Res Commun* 485: 388–394. https://doi.org/10.1016/j.bbrc.2017.02.067
27. Wang T, Yu Q, Li J, et al. (2017) O-GlcNAcylation of fumarase maintains tumor growth under glucose deficiency. *Nat Cell Biol* 19: 833–843. https://doi.org/10.1038/ncb3562
28. Uchiumi F, Larsen S, Masumi A, et al. (2013) The putative implications of duplicated GGAA-motifs located in the human interferon regulated genes (ISGs). In: *Genomics I-humans, animals and plants*, 87–105.
29. Uchiumi F, Larsen S, Tanuma S (2015*)* Transcriptional regulation of the human genes that encode DNA repair- and mitochondrial function-associated proteins. In: *Advances in DNA repair*, 129–167. https://doi.org/10.5772/59588
30. Yang C, Bolotin E, Jiang T, et al. (2007) Prevalence of the initiator over the TATA box in human and yeast genes and identification of DNA motifs enriched in human TATA-less core promoters. *Gene* 389: 52–65. https://doi.org/10.1016/j.gene.2006.09.029
31. Hamada H, Yamamura M, Ohi H, et al. (2019) Characterization of the human zinc finger nfx-1-type containing 1 gene promoter and its response to 12-*O*-tetradecanoyl-13-acetate in HL-60 cells. *Int J Oncol* 55: 869–974. https://doi.org/10.3892/ijo.2019.4860
32. Uchiumi F, Arakawa J, Iwakoshi S, et al. (2016) Characterization of the 5'-flanking region of the human DNA helicase B (*HELB*) gene and its response to *trans*-resveratrol. *Sci Rep* 6: 24510. https://doi.org/10.1038/srep24510

33. Uchiumi F, Katsuda C, Akui M, et al. (2020) Effect of the natural compound trans-resveratrol on human *MCM4* gene transcription. *Oncol Rep* 44: 283–292. https://doi.org/10.3892/or.2020.7598
34. Wünschiers R (2012) Carbohydrate metabolism and citrate cycle. In: *Biochemical pathways: An atlas of biochemistry and molecular biology*, 37–58.
35. Jahn M, Jahn D (2012) Electron transfer reactions and oxidative phosphorylation. In: *Biochemical pathways: An atlas of biochemistry and molecular biology*, 183–188.
36. Goldschmidt-Reisin S, Kitakawa M, Herfurth E, et al. (1998) Mammalian mitochondrial ribosomal proteins. N-terminal amino acid sequencing, characterization, and identification of corresponding gene sequences. *J Biol Chem* 273: 34828–34836. https://doi.org/10.1074/jbc.273.52.34828
37. Lightowlers RN, Chrzanowska-Lightowlers ZM (2013) Human pentatricopeptide proteins: Only a few and what do they do? *RNA Biol* 10: 1433–1438. https://doi.org/10.4161/rna.24770
38. Muley P, Olinger A, Tummala H (2015) 2-Deoxyglucose induces cell cycle arrest and apoptosis in colorectal cancer cells independent of its glycolysis inhibition. *Nutr. Cancer* 67: 514–522. https://doi.org/10.1080/01635581.2015.1002626
39. Seyfried TN, Shelton LM (2010) Cancer as a metabolic disease. *Nutr. Metab* 7: 7. https://doi.org/10.1186/1743-7075-7-7
40. Gomes AP, Price NL, Ling AJ, et al. (2013) Declining NAD^+ induces a pseudohypoxic state disrupting nuclear-mitochondrial communication during aging. *Cell* 155: 1624–1638. https://doi.org/10.1016/j.cell.2013.11.037
41. Chu B, Wu T, Miao L, et al. (2015) MiR-181a regulates lipid metabolism via IDH1. *Sci Rep* 5: 8801. https://doi.org/10.1038/srep08801
42. Liu, WS, Chan SH, Chang HT, et al. (2018) Isocitrate dehydrogenase 1-snail axis dysfunction significantly correlates with breast cancer prognosis and regulates cell invasion ability. *Breast Cancer Res* 20: 25. https://doi.org/10.1186/s13058-018-0953-7
43. Tanaka H, Sasayama T, Tanak K, et al. (2013) MicroRNA-183 upregulates HIF-1α by targeting isocitrate dehydrogenase 2 (IDH2) in glioma cells. *J Neurooncol* 111: 273–283. https://doi.org/10.1007/s11060-012-1027-9
44. Han L, Zhang Y, Zhao B, et al. (2022) MicroRNA 101 attenuated NSCLC proliferation through IDH2/HIFα axis suppression in the Warburg effect. *Oxid Med Cell Longev* 2022: 4938811. https://doi.org/10.1155/2022/4938811
45. Metallo CM, Gameiro PA, Bell EL, et al. (2011) Reductive glutamine metabolism by IDH1 mediates lipogenesis under hypoxia. *Nature* 481: 380–384. https://doi.org/10.1038/nature10602
46. Widłak W, Vydra N, Dudaladava V, et al. (2007) The GC-box is critical for high level expression of the testis-specific Hsp70.2/Hst70 gene. *Acta Biochim Pol* 54: 107–112.
47. Bajpai R, Nagaraju GP (2017) Specificity protein 1: Its role in colorectal cancer progression and metastasis. *Crit Rev Oncol Hematol* 113: 1–7. https://doi.org/10.1016/j.critrevonc.2017.02.024
48. Kim SY, Park JW (2010) Modulation of hypoxia-inducible factor-1α expression by mitochondrial $NADP^+$-dependent isocitrate dehydrogenase. *Biochimie* 92: 1908–1913. https://doi.org/10.1016/j.biochi.2010.08.004
49. Li X, Liu X, Xu Y, et al. (2014) KLF5 promotes hypoxia-induced survival and inhibits apoptosis in non-small cell lung cancer cells via HIF-1α. *Int J Oncol* 45: 1507–1514. https://doi.org/10.3892/ijo.2014.2544

50. Uchiumi F, Miyazaki S, Tanuma S (2011) The possible functions of duplicated *ets* (GGAA) motifs located near transcription start sites of various human genes. *Cell Mol Life Sci* 68: 2039–2051. https://doi.org/10.1007/s00018-011-0674-x
51. Shen Y, Kapfhamer D, Minnella AM, et al. (2017) Bioenergetic state regulates innate inflammatory responses through the transcriptional co-repressor CtBP. *Nat Commun* 8: 624. https://doi.org/10.1038/s41467-017-00707-0
52. Kim JH, Youn HD (2009) C-terminal binding protein maintains mitochondrial activities. *Cell Death Differ* 16: 584–592. https://doi.org/10.1038/cdd.2008.186
53. Hu R, Sharma SM, Bronisz A, et al. (2007) Eos, MITF, and PU.1 recruit corepressors to osteoclast-specific genes in committed myeloid progenitors. *Mol Cell Biol* 27: 4018–4027. https://doi.org/10.1128/MCB.01839-06
54. Yamamoto H, Kihara-Negishi F, Yamada T, et al. (1999) Physical and functional interactions between the transcription factor PU.1 and the coactivator CBP. *Oncogene* 18: 1495–1501. https://doi.org/10.1038/sj.onc.1202427
55. Calvert AE, Chalastainis A, Wu Y, et al. (2017) Cancer-associated IDH1 promotes growth and resistance to targeted therapies in the absence of mutation. *Cell Rep* 19: 1858–1873. https://doi.org/10.1016/j.celrep.2017.05.014
56. Jo SH, Son MK, Koh HJ, et al. (2001) Control of mitochondrial redox balance and cellular defense against oxidative damage by mitochondrial $NADP^+$-dependent isocitrate dehydrogenase. *J Biol Chem* 276: 16168–16176. https://doi.org/10.1074/jbc.M010120200
57. Son MJ, Ryu JS, Kim JY, et al. (2017) Upregulation of mitochondrial NAD^+ levels impairs the clonogenicity of $SSEA1^+$ glioblastoma tumor-initiating cells. *Exp Mol Med* 49: e344. https://doi.org/10.1038/emm.2017.74
58. Tummala KS, Gomes AL, Yilmaz M, et al. (2014) Inhibition of de novo NAD^+ synthesis by oncogenic URI causes liver tumorigenesis through DNA damage. *Cancer Cell* 26: 826–839. https://doi.org/10.1016/j.ccell.2014.10.002
59. Molenaar RJ, Maciejewski JP, Wilmink JW, et al. (2018) Wild-type and mutated IDH1/2 enzymes and therapy responses. *Oncogene* 37: 1949–1960. https://doi.org/10.1038/s41388-017-0077-z
60. Heo J, Lim J, Lee S, et al. (2017) Sirt1 regulates DNA methylation and differentiation potential of embryonic stem cells by antagonizing Dnmt3l. *Cell Rep* 18: 1930–1945. https://doi.org/10.1016/j.celrep.2017.01.074
61. Uchiumi F, Arakawa J, Takihara Y, et al. (2018) A new insight into the development of novel anti-cancer drugs that improve the expression of mitochondrial function-associated genes. In: *Mitochondrial diseases*, 107–134. https://doi.org/10.5772/intechopen.71095
62. Weinberg SE, Chandel NS (2015) Targeting mitochondria metabolism for cancer therapy. *Nat Chem Biol* 11: 9–15. https://doi.org/10.1038/nchembio.1712
63. Uchiumi F, Sato A, Asai M, et al. (2020) An NAD^+ dependent/sensitive transcription system: Toward a novel anti-cancer therapy. *AIMS Mol Sci* 7: 12–28. https://doi.org/10.3934/molsci.2020002

Appendix

Supplementary Figure 1. BLAST search program for the upstream sequence 153-bp region of the mouse Idh1 gene transcript variant 2 (in NC_000067.7) and the 154-bp.